Journal of Intelligent Material Systems and Structures

Article

Journal of Intelligent Material Systems and Structures
24(17) 2074–2083

DOI: 10.1177/1045389X12453964
jim.sagepub.com
SAGE

Low-velocity impact damage monitoring of a sandwich composite wing

Yingtao Liu and Aditi Chattopadhyay

Abstract

Impact damage has been identified as a critical form of defect that constantly threatens the reliability of composite structures, such as those used in aircrafts and naval vessels. Low-energy impacts can introduce barely visible damage and cause structural degradation. Therefore, efficient structural health monitoring methods, which can accurately detect, quantify, and localize impact damage in complex composite structures, are required. In this article, a novel damage detection methodology is demonstrated for monitoring and quantifying the impact damage propagation. Statistical feature matrices, composed of features extracted from the time and frequency domains, are developed. Kernel principal component analysis is used to compress and classify the statistical feature matrices. Compared with traditional principal component analysis algorithm, kernel principal component analysis method shows better feature clustering and damage quantification capabilities. A new damage index, formulated using the Mahalanobis distance, is defined to quantify impact damage. The developed methodology has been validated using low-velocity impact experiments with a sandwich composite wing.

Keywords

Low-velocity impact damage, structural health monitoring, kernel principal component analysis, macro fiber composite, damage quantification, damage index, active sensing, sandwich composite wing

Introduction

Over the past decade, carbon fiber-reinforced plastic (CFRP) materials have been widely used in aerospace, naval, mechanical, and infrastructure applications. For example, CFRP has been used in both secondary and primary structures of numerous commercial and military airplanes. However, one of the limiting factors to the use of laminated composites is their internal damage state. Although design criteria for such applications include damage tolerance requirements that specify the ability of a structure to operate safely with initial defects, in-service damage resistance and repair remain a major issue. Low-velocity impacts can cause serious damage to CFRP composites even when the damage is not readily visible. Therefore, efficient structural health monitoring (SHM) techniques are required for detection and monitoring of such damage in order to accurately predict structural integrity and residual useful life, which in turn will improve safety, extend life, reduce maintenance, and minimize downtime of complex composite systems. Although in the past few years there has been an increased interest in the development of robust SHM systems, the implementation of such a system requires a multidisciplinary research effort in a number of areas. This includes novel sensors and sensing methodologies, improved interrogation techniques that better diagnose current state and conditions, robust approaches to characterize material behavior and predict future failures, and life assessment techniques integrated with high-fidelity modeling (Farrar and Lieven, 2007; Giurgiutiu, 2008; Liu et al., 2010, 2011; Lynch, 2007; Raghavan and Cesnik, 2007; Yekani Fard et al., 2011a, 2011b, 2012).

Impact has been the subject of many experimental and analytical investigations. Sources of low-velocity impacts include tool drop, runway debris, collision with vehicles, and so on. The internal damage state after a low-velocity impact in CFRP composites can be

School for Engineering of Matter, Transport and Energy, Arizona State University, Tempe, AZ, USA

Corresponding author:
Yingtao Liu, School for Engineering of Matter, Transport and Energy, Arizona State University, Tempe, AZ 85287, USA.
Email: yliu158@asu.edu

complex and multimodal, including matrix cracking, delaminations, and fiber breakage. The impact damage can propagate under service loading leading to catastrophic structural failure. Therefore, it is critical to develop accurate and robust SHM methodologies to detect and monitor the damage initiation due to low-velocity impacts.

Advanced sensing and associated signal analysis/interpretation approaches have been well developed to monitor impacts on composite structures with simple geometries. Meo and Zumpano (2005) developed an in situ damage detection and identification methodology using piezoelectric sensors and guided wave propagation approaches. Moll et al. (2010) reported a multisite damage localization approach applicable to anisotropic wave propagation that did not assume any simplifications regarding to anisotropic wave propagation. Hiche et al. (2011) developed a strain amplitude–based algorithm for impact localization on composite laminates using fiber Bragg grating (FBG) sensors. Liu et al. (2012) presented a time–frequency-based damage detection and quantification method using matching pursuit decomposition algorithm. However, due to the complex damage mechanisms, most of the published data-driven approaches only validated the methodologies on plate-like or sandwich composite structures. Due to the associated challenges, very limited work has been reported on application to complex geometries and real applications.

Obtaining a proper feature representation of the damage state from the sensing data is a fundamental problem in SHM. Generally, not all the original features are beneficial for damage detection and classification. Some of the features include a significant amount of noise and will negatively influence the performance of SHM system. Therefore, it is essential to remove the noisy features or derive some new features from original data space, so that only the necessary information is retained for damage classification, quantification, and prognosis. Traditionally, linear feature extraction and selection are conducted in the original input space. Nonlinear relationships cannot be extracted from the original dataset. For example, only features from time domain or frequency domain are considered in some of the lead zirconate titanate (PZT)–based active sensing approaches (Sohn et al., 2001; Su et al., 2006; Tang et al., 2011). However, the nonlinear structural degradation process may not be fully represented by time or frequency domain features. It is necessary to develop robust feature extraction/selection methodologies to represent the multiscale structural damage in heterogeneous material systems.

This article extends the damage quantification work on composite wing sections using FBG sensors initiated by Seaver et al. (2010). A new feature selection methodology for impact damage detection and quantification using kernel method and a guided wave–based active sensing approach is developed. The effects of statistical feature selection using kernel principal component analysis (KPCA) from the time and frequency domains are studied. A robust SHM feature is extracted using KPCA to represent the low-velocity impact damage on a composite sandwich wing structure. A damage index based on the Mahalanobis distance is used to quantify the damage. The methodology is applied to a composite wing of an unmanned aerial vehicle (UAV).

The remainder of the article is organized as follows. Section "Statistical feature extraction" introduces the mathematical formulation of feature extraction and damage quantification. This is followed by experimental procedure in section "Experiments," which presents details of the low-velocity impact tests and nondestructive tests using flash thermography. The results from impact detection and quantification are presented in section "Results and discussion."

Statistical feature extraction

Selection of appropriate features, which are sensitive to damage but robust to noise, is a key issue in SHM. Statistical features have been demonstrated to be useful to represent damage in complex engineering structures (Sohn et al., 2001). One of the most popular statistical methods is principal component analysis (PCA). A PCA-based multivariate statistical technique integrated with Q and T^2 measures was able to distinguish cracks in a steel plate and identify an added mass on an aircraft turbine blade (Mujica et al., 2011). The method has been proven to be useful in both the low-frequency range using vibration-based approaches and high-frequency range using guided wave–based active sensing approaches. However, PCA can only extract linear features. Because most complex engineering systems are associated with nonlinearity, nonlinear features can be more useful for damage detection and quantification. A nonlinear statistical feature extraction method is used in this study to identify and quantify low-velocity impact damage in a composite wing.

Statistical analysis using KPCA

KPCA is a nonlinear extension of PCA and can be used to extract the nonlinear relation among variables (Cao et al., 2007; Scholkopf et al., 1999). In KPCA, a nonlinear kernel function is used instead of a linear function; the PCA can now be performed in a high-dimensional space that is nonlinearly related to the

input space. Assuming the input data is mapped into the centered feature space Φ, we have

$$\sum_{j=1}^{N} \Phi(x_j) = 0 \tag{1}$$

The covariance matrix is defined as

$$\bar{C} = \frac{1}{N} \sum_{j=1}^{N} \Phi(x_j) \Phi(x_j)^T \tag{2}$$

The eigenvalues λ and eigenvectors V satisfy

$$\lambda V = \bar{C} V \tag{3}$$

It must be noted that the solutions for V that satisfy equation (3) lie in $\Phi(x_j)$ ($j = 1, \ldots, N$). Therefore, we can write

$$\lambda \left(\Phi(x_j) \cdot V \right) = \left(\Phi(x_j) \cdot \bar{C} V \right) \tag{4}$$

and

$$V = \sum_{j=1}^{N} \propto_j \Phi(x_j) \tag{5}$$

where $\propto_j$ ($j = 1, \ldots, N$) are the coefficients. The kernel matrix K can be defined as

$$k_{ij} = \Phi(x_i)^T \Phi(x_j) = \Phi(x_i) \cdot \Phi(x_j) \tag{6}$$

Based on the application, different kernel functions, such as sigmoid kernels and polynomial kernels, can be selected to get the best performance. In this article, a Gaussian kernel function is used to nonlinearly map the input data to the high-dimensional space. The N-dimensional Gaussian kernel is defined as

$$K_N \left(\vec{x}, \sigma \right) = \frac{1}{\left(\sqrt{2\pi\sigma} \right)^N} e^{-\frac{|\vec{x}|}{2\sigma^2}} \tag{7}$$

where σ determines the width of the Gaussian kernel. The new eigenvalues obtained from the KPCA analysis are used as the new feature vectors for the impact damage quantification.

Mahalanobis distance–based damage index

The low-velocity impacts are quantified using a Mahalanobis distance–based damage index. The use of the Mahalanobis distance has been demonstrated as a useful parameter for feature classification and quantification (Sohn, 2007). Two feature vectors $\vec{x}$ and $\vec{y}$ are assumed to have $\vec{x}\vec{y}$ the same distribution with the covariance matrix S. The Mahalanobis distance D^M is expressed as

$$D^M = \sqrt{D} = \sqrt{\left(\vec{x} - \vec{y} \right)^T S^{-1} \left(\vec{x} - \vec{y} \right)} \tag{8}$$

where S^{-1} represents the inverse of the covariance matrix S. The Mahalanobis distance is used to define a new damage index for impact damage quantification in this article. Denoting the KPCA feature vector at the ith damage state $\vec{F}_i$ and the KPCA feature vector at the healthy state $\vec{F}_h$, the damage index DI_i corresponding to the ith damage state can be defined as

$$DI_i = \frac{D^M \left(\vec{F}_i, \vec{F}_h \right)}{D^M \left(\vec{F}_h, \vec{F}_h \right)} \tag{9}$$

Experiments

A sandwich composite UAV wing was used as the test article to assess the damage propagation due to multiple impacts. The wing is composed of four layers of carbon fiber fabrics; two layers were made from woven fiber fabrics (C282 carbon fabrics) and two layers were made from unidirectional fiber fabrics (3K T300 5″ uni tape). The layup of the composite skin is ±45° woven/0° uni/0° uni/±45° woven. The epoxy resin used is MGS L285 (HEXION Inc.) with MGS H287S (HEXION Inc.) hardener. There is an aluminum core at the center, which can be used to connect the wing to the UAV fuselage. The rest of the wing has a foam core made from Last-A-Foam (General Plastics Inc.). The cross section of the wing has an airfoil shape. The geometry and cross section of the wing is shown in Figure 1.

A series of impact tests were conducted to investigate the effects of low-velocity impacts on the composite wing. A pair of customized wing fixtures was fabricated to clamp the wing. The experimental setup is shown in Figure 2(a). A swing arm impact system is used in the experiment. The diameter of the impactor head is approximately 32 mm. Both the impact force and velocity were recorded to estimate the impact energy deposited in the test article. The impact force was measured using a dynamic load cell (Model: 1061V4, Dytran Inc.), and the velocity and position of the swing arm were measured using a rotary encoder. By running

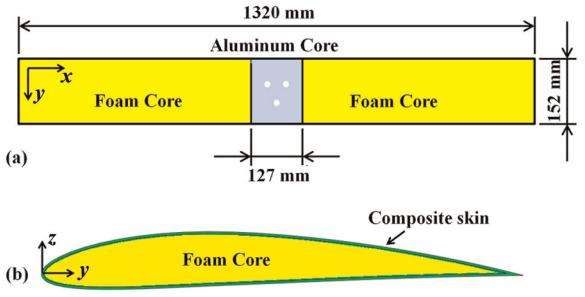

Figure 1. Geometry and cross section of composite wing.

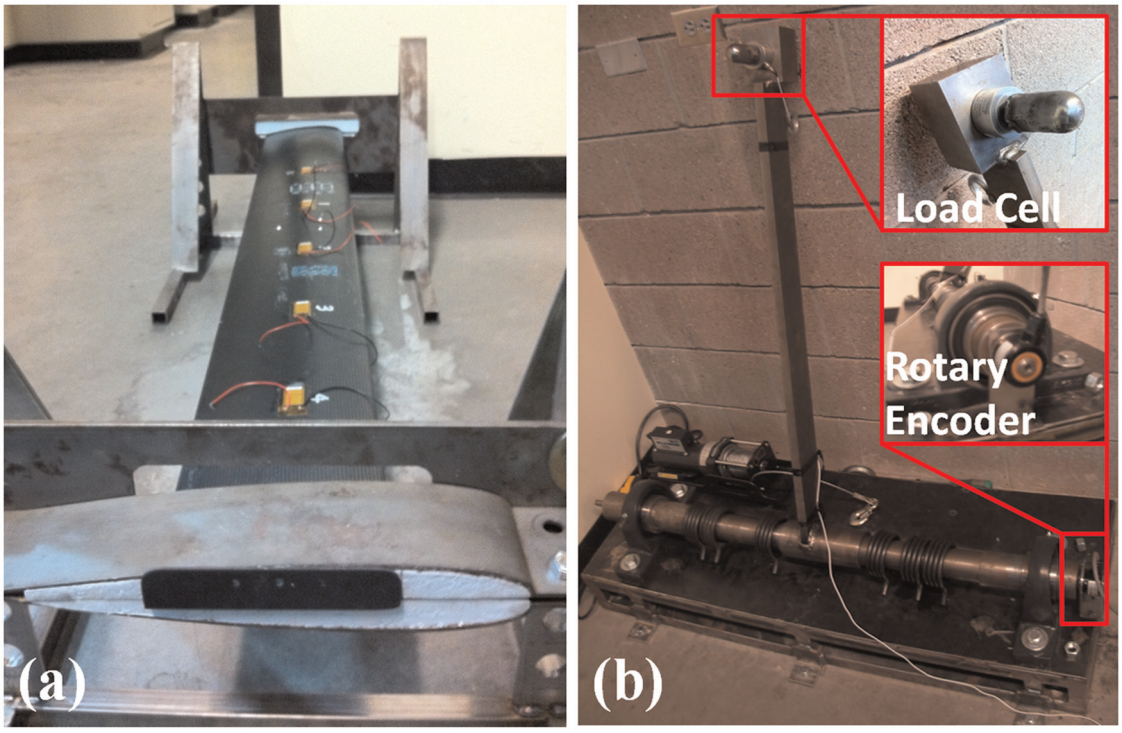

Figure 2. (a) Experimental setup: composite wing in the fixture and (b) low-velocity impact system.

several trial tests, an appropriate initial height of the impact head was determined to ensure damage of the foam core but not the composite skin. The impact energy is about 11 J for each impact test.

The impact area was divided into eight sections. A total of 10 impact tests were conducted. The exact impact locations are shown in Figure 3. No visible damage was observed on the composite skin during the first eight impacts. However, the 9th and 10th impacts introduced several visible dents on the composite skin, as shown in Figure 4.

Nondestructive tests using the flash thermography (Model: EchoTherm; Thermal Wave Imaging Inc.) were conducted to visualize the extent of damage. Flash thermography utilizes high-density flash heat generated by infrared heat lamps to excite the specimen with thermal radiation. Two infrared cameras record the thermal images with respect to time to evaluate the change in temperature field over time. Structural damage and imperfections can be differentiated from undamaged material due to their difference in local thermal diffusivity. Flash thermography images were taken before and after each impact, as shown in Figure 5. Prior to impact testing, no structural defect was detected because the temperature in the test field decays at a constant rate. However, after each impact, the red spots in the flash thermography images demonstrate the varying thermal diffusivity at the impact area. This indicates damage propagation and structural degradation caused by the series of low-velocity impacts. After

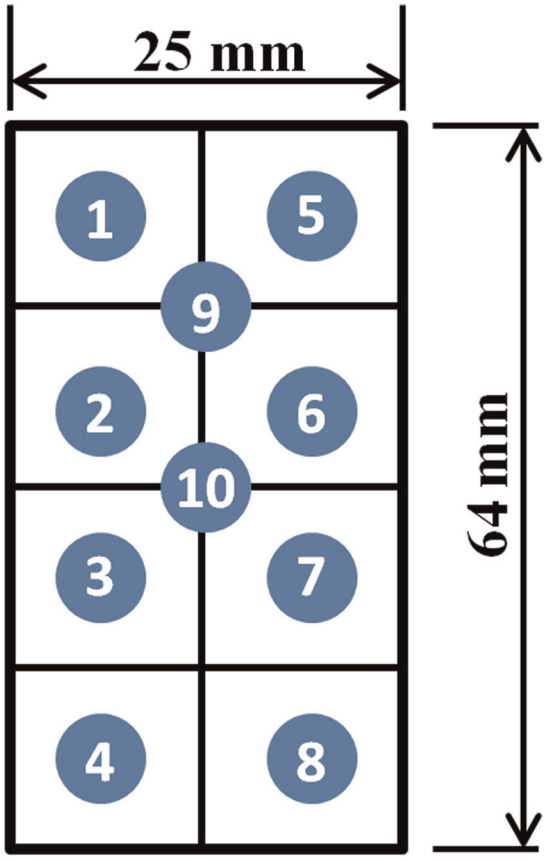

Figure 3. Impact sequence during experiment.

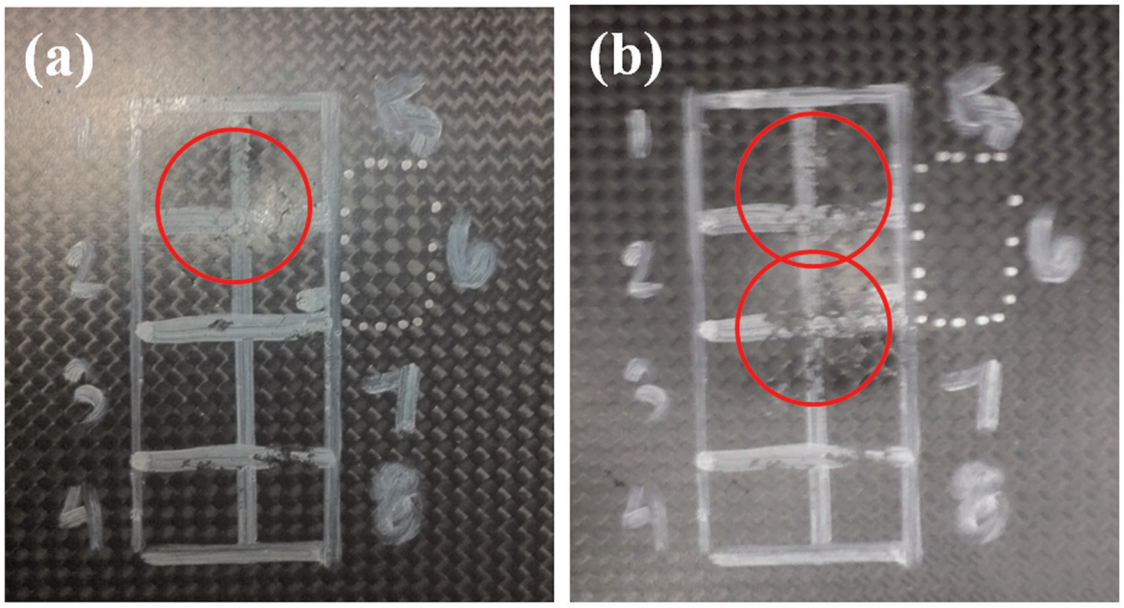

Figure 4. Visible damages in composite skin after impacts 9 and 10: (a) damage after impact 9 and (b) damage after impact 10.

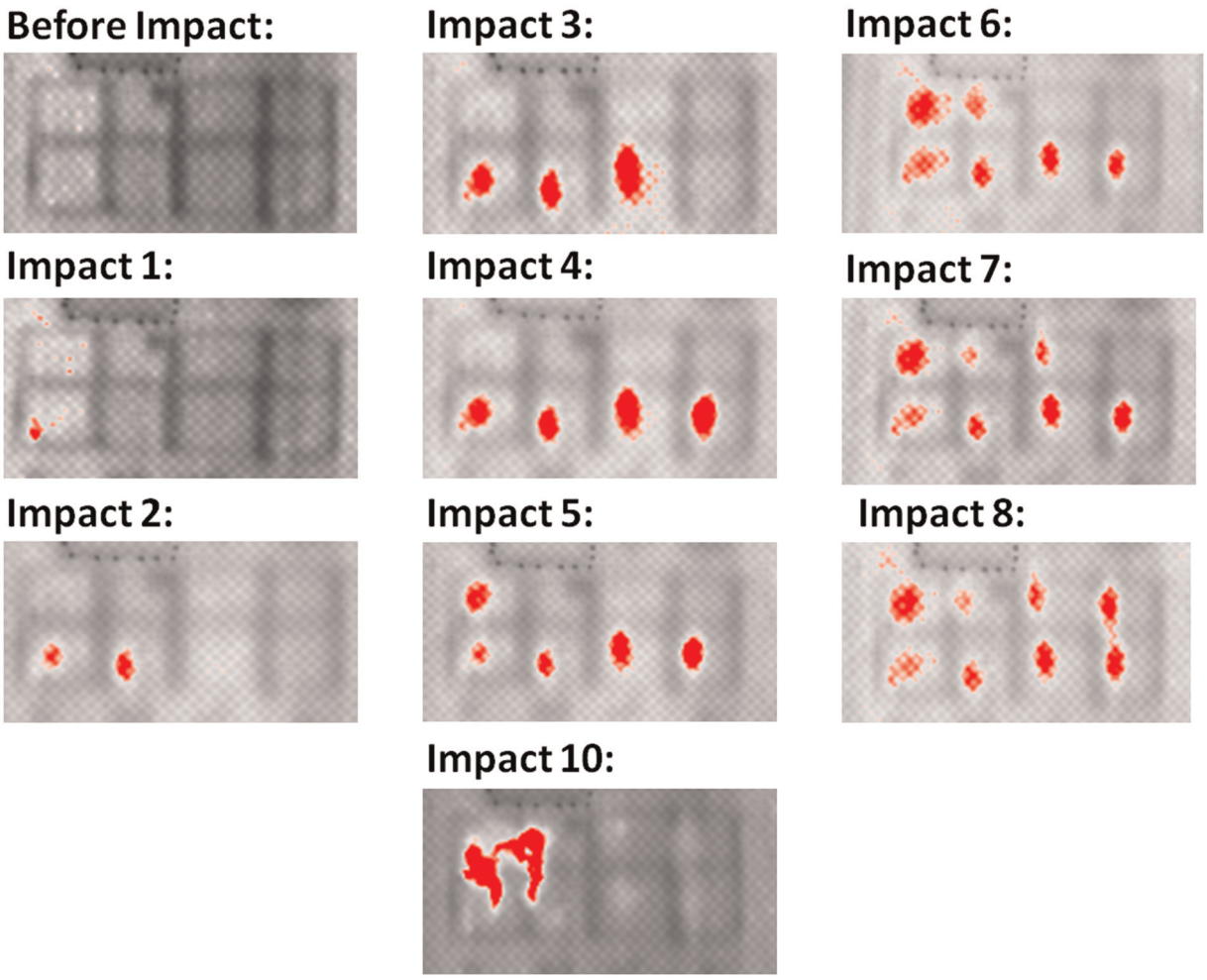

Figure 5. Flash thermography images of the damage area before and after impact tests 1–8 and 10.

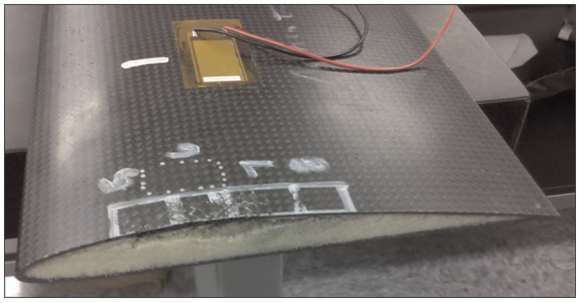

Figure 6. Composite wing autopsy after impact test 10.

impacts 1–8, the flash thermography images represent the estimated damage sizes introduced during experiments. After impacts 9 and 10, although structural damages have been visible, the flash thermography images can still be used to measure the damage sizes. The sizes have been used to represent the severity of impact damages. More details are discussed in section "Results and discussion."

A wing autopsy test was conducted after the 10th impact to diagnose the exact nature of the damage in the composite wing. Multiple types of damage including foam cracking, debonding between foam core and composite skin, and fiber breakage and delaminations in the composite skin were detected, as shown in Figure 6.

To detect and quantify the impact damage, a guided wave–based active sensing approach using macro fiber composite (MFC) transducers is used in this article. Two MFC transducers were surface instrumented on the composite wing. The positions of MFCs are shown in Figure 7. A 4.5-cycle cosine-windowed tone burst wave was used as the excitation signal. The excitation waveform was generated using the Ni 5412 (National Instruments) waveform generator, and the Lamb wave signals were captured using the NI 5105 (National Instruments) digitizer at the sampling frequency of 20 MHz. In order to optimize the central frequency of the excitation signal, several signals were generated using central frequencies varying from 10 to 300 kHz in 10-

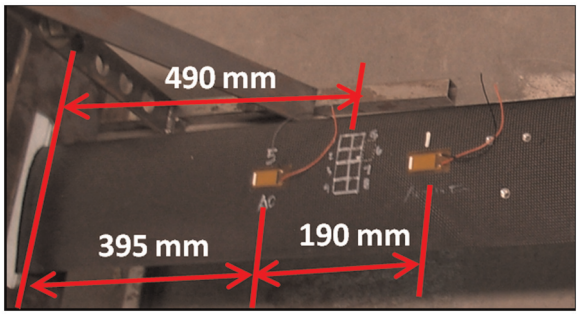

Figure 7. Surface instrumented MFC transducers for active sensing.
MFC: macro fiber composite.

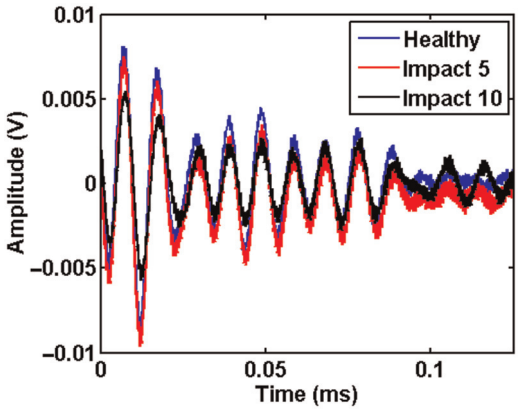

Figure 8. Original sensing signals from healthy state and impacts 5 and 10.

kHz increments. Ten observations were recorded at each frequency, and the sensor signals were averaged from these observations to reduce the sampling error. After preliminary tests and signal processing, the optimal frequency selected was 100 kHz. The sensor signals were collected at the healthy state and following the 5th and 10th impacts, as shown in Figure 8.

Results and discussion

To monitor the condition of the composite sandwich wing, nine statistical features of the MFC sensor signals in the time and frequency domains are extracted to represent the characteristics of damage. At each damage state, every observation provides one feature vector, denoted as $\{\bar{F}_i | i = 1, \ldots, 9\}$. Because 100 observations are recorded at each damage state, 100 statistical feature vectors can be obtained. First, five statistical features are extracted from the time domain of the sensor signals. These features are root mean square (RMS), variance, Kurtosis, peak value, and peak-to-peak value. Using fast Fourier transform (FFT) and Hilbert transform (HT), the MFC sensor signals are transformed to the frequency domain. The power spectrum energy is calculated as the sum of the frequency amplitude using FFT. The Hilbert spectrum is calculated using HT. The maximum power spectrum density (PSD) and maximum HT amplitude are also considered as statistical features. A detailed definition of each statistical feature is presented in Table 1.

The extracted statistic features are shown in Figure 9. It is noted that these features can provide rough trends of structural degradation. However, these feature trends are not constant, and it is difficult to estimate which features are more sensitive to impact damage. In addition, some of these original statistical features repeatedly demonstrate similar sensing information. Briefly stated, advanced techniques are required to extract more robust features and reduce the redundant features.

Table 1. Definition of the statistical features in time and frequency domains.

Name	Definition
RMS	$x_{rms} = \sqrt{\frac{1}{M}\sum_{i=1}^{M}\lvert x_i\rvert}$
Variance	$Var_x = \frac{1}{M-1}\sum_{i=1}^{M}(x_i - \bar{x})^2$
Kurtosis	$Kur_x = \frac{1}{M}\sum_{i=1}^{M} x_i^4$
Peak value	$P_x = \lvert\max(x)\rvert$
Peak-to-peak value	$PP_x = \lvert\max(x)\rvert + \lvert\min(x)\rvert$
PSD	$\varphi(\omega) = \left\lvert\frac{1}{\sqrt{2\pi}}\sum_{i=-\infty}^{\infty} x_i e^{-i\omega n}\right\rvert^2$
Signal energy	$E = \int_0^F \varphi(f)df$
Maximum HT amplitude	$HT_{max} = \max\left(\frac{1}{\pi}\int_{-\infty}^{\infty}\frac{x(\tau)}{\tau - t}d\tau\right)$
HT area	$A = \int_0^F HT\,df$

RMS: root mean square; PSD: power spectrum density; HT: Hilbert transform.

For the purpose of comparison, both the KPCA and PCA techniques are applied to the original statistical features $\{\bar{F}_m | m = 1, \ldots, 9\}$. Every 10 feature vectors are combined to build the feature matrix for the PCA and KPCA analyses. The feature matrix can be expressed as $F_{mn} | m = 1, \ldots, 9, n = 1, \ldots, 10$, where m is the number of feature in each feature vector and n is the number of observations in each feature matrix.

The key issue in the KPCA algorithm is to transform the input features into a high-dimensional feature space using nonlinear mapping. In this article, the nonlinear mapping is conducted using the kernel function as shown in equations (6) and (7). The first three principal components using KPCA and PCA methods are extracted at three states: the healthy state, the state following the 5th impact, and the state following the 10th impact. The cluster analysis results are shown in Figures 10 and 11. The traditional PCA algorithm can extract and select features in the original input space, but cannot handle the nonlinear relationships in the input features well. This indicates the lack of a clear separation between damage states using the PCA method. However, the KPCA representations in Figure 11 show clear separation among the three states. This demonstrates that KPCA can extract the higher order and nonlinear information that is more useful to demonstrate the effects of low-velocity impact to the composite wing. Furthermore, more robust damage quantification results can be obtained when the KPCA features are used.

The Mahalanobis distance–based damage index defined in equation (8) is used to quantify the extent of the low-velocity impact damage. Ten KPCA feature sets at each damage state are obtained using the developed algorithm. The average features calculated from these feature sets are used as the input to quantify the damage. As shown in Figure 12, the low-velocity damage propagates almost at a constant rate during the first eight impact events. However, the damage propagation is much faster during the last two impacts. This can be explained as follows. During the first eight impacts, the impact head hits a new section on the wing surface, as shown in Figure 3, and since each impact introduces the same amount of energy into the wing, the propagation rate is consistent. The last two impacts were between multiple previous impact sections. Although there was no visible surface damage shown after the first eight impacts, the wing foam cracked and there were delaminations between the composite skin and foam. When these areas were further impacted, the damage severity increased significantly even though the impact energy was still the same. The total delamination sizes after each impact are shown in Figure 12. The defined damage index has good agreement with the delamination size. This result proves that the proposed damage quantification algorithm can be used to represent the delamination damage in the composite UAV wing. In addition, it illustrates the critical nature of repetitive low-velocity impact damage on composite wing, which may lead to catastrophic failure.

Conclusion

An impact damage monitoring and quantification methodology using KPCA algorithm is developed in this article. Statistical features are extracted from the sensor signals in the time and frequency domains. Choosing an appropriate kernel function, the statistical features are mapped to a high-dimensional space for feature clustering. The kernel eigenvalue obtained from the original statistical feature datasets represents the damage propagation caused by impacts, which are considered as new feature datasets for damage quantification. Redundant features are compressed during the KPCA analysis. A novel Mahalanobis distance–based damage index is defined to quantify the impact damage.

Low-velocity impact experiments were conducted on a sandwich composite wing to validate the developed methodology. MFC-based active sensing was used for damage detection. After each impact, flash thermography images were taken to detect the presence of subsurface (invisible) damage. A wing autopsy was conducted after the last impact to examine the exact nature of the damage in the composite wing. Multiple types of damage including fiber breakage, foam cracking, delaminations in the composite skin, and delaminations between composite skin and foam core were detected. By studying the MFC sensor data, the damage quantification

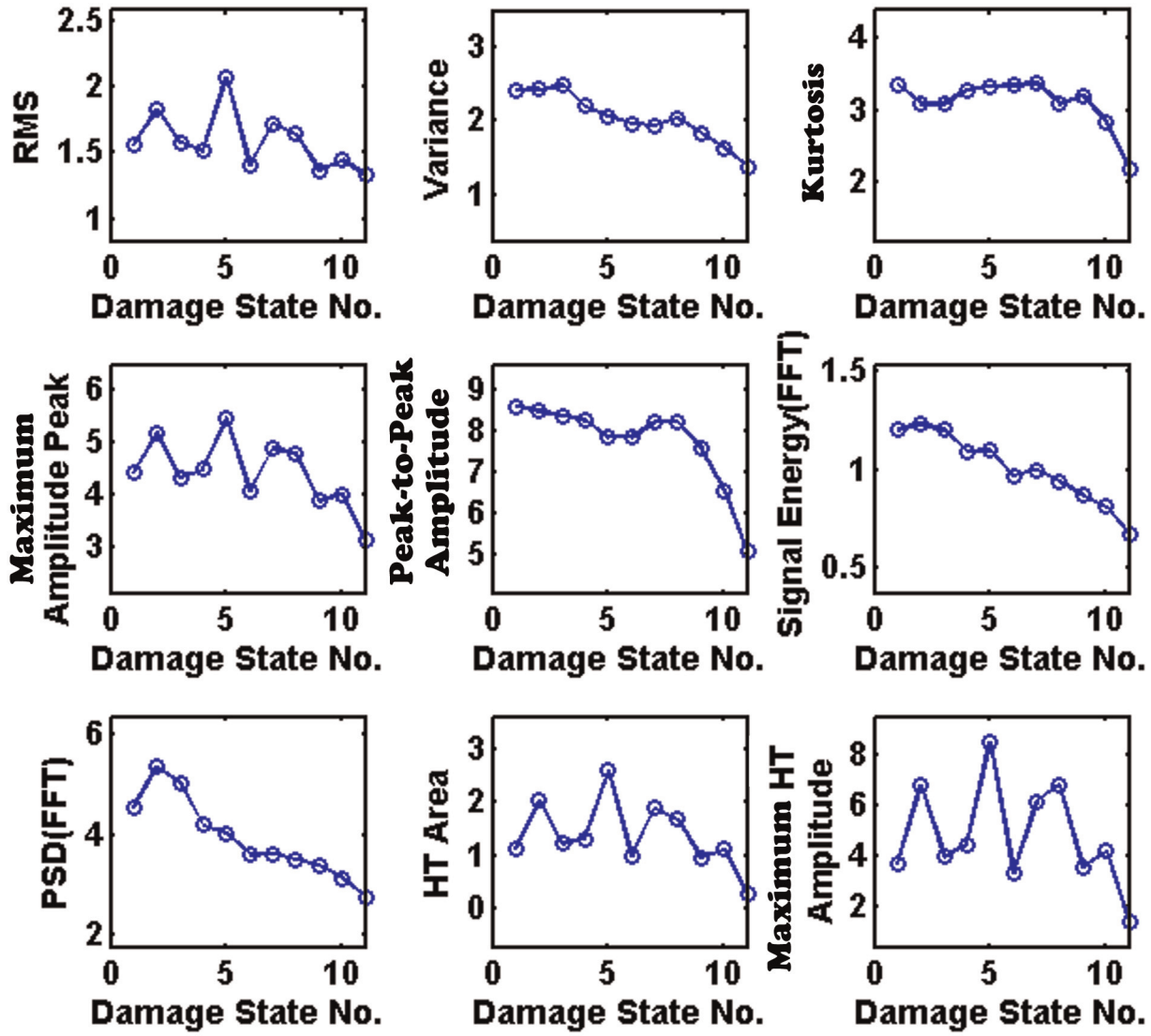

Figure 9. Statistical features extracted from the time and frequency domains.
PSD: power spectrum density; FFT: Fourier transform; RMS: root mean square; HT: Hilbert transform.

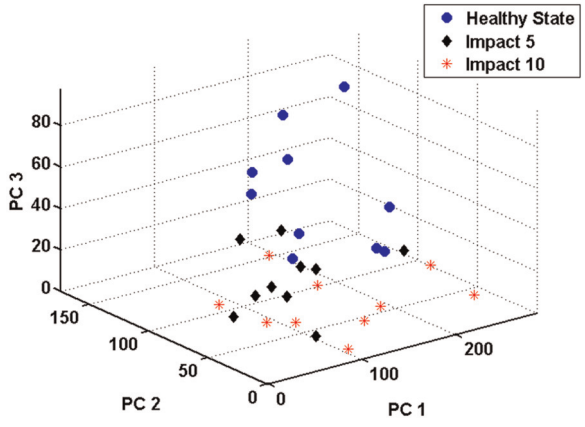

Figure 10. Typical PCA features for healthy state and impacts 5 and 10.
PCA: principal component analysis.

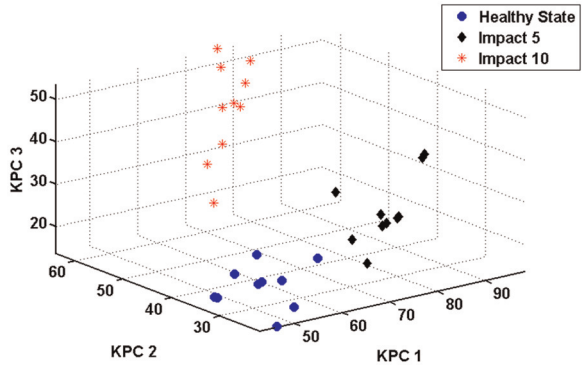

Figure 11. Typical KPCA features for healthy state and impacts 5 and 10.
KPCA: kernel principal component analysis.

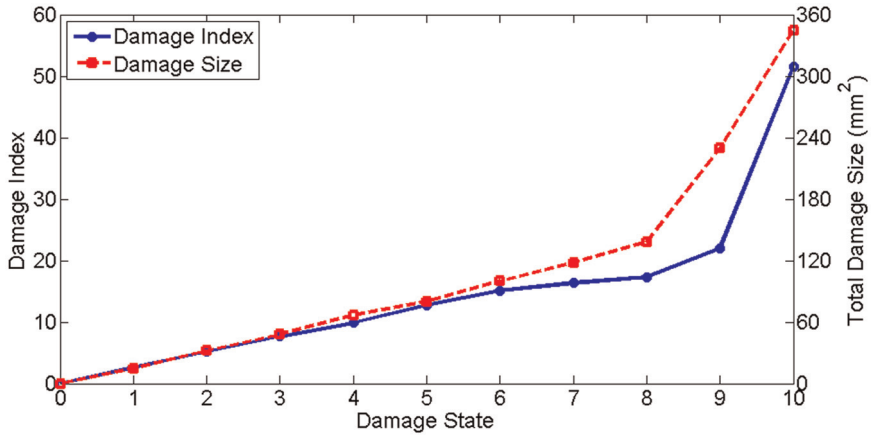

Figure 12. Damage quantification using the Mahalanobis distance–based damage index.

results show steady structural degradation after the initial eight impacts, followed by rapid damage progression over the last two impacts. There is good agreement between the estimated damage index and the real damage sizes measured using flash thermography system.

Acknowledgment

The authors gratefully appreciate Dr Mark Seaver from Naval Research Laboratory for providing the sandwich composite wing and advising the impact experiments.

References

Cao B, Shen D, Sun JT, et al. (2007) Feature selection in a kernel space. In: *Proceedings of the 24th international conference on machine learning*, Corvallis, OR, 20–24 June, pp. 121–128. DOI:10.1145/1273496.1273512.

Farrar CR and Lieven NAJ (2007) Damage prognosis: the future of structural health monitoring. *Philosophical Transactions of the Royal Society A-Mathematical Physical and Engineering Sciences* 365: 623–632.

Giurgiutiu V (2008) *Structural Health Monitoring with Piezoelectric Wafer Active Sensors*. Amsterdam: Elsevier Inc.

Hiche C, Ceolho C and Chattopadhyay A (2011) A strain amplitude-based algorithm for impact localization on composite laminates. *Journal of Intelligent Material Systems and Structures* 22(17): 2061–2067.

Liu Y, Kim SB, Chattopadhyay A, et al. (2011) Application of system identification techniques to health monitoring of on-orbit satellite boom structures. *Journal of Spacecraft and Rockets* 48(4): 589–598.

Liu Y, Mohanty S and Chattopadhyay A (2010) Condition based structural health monitoring and prognosis of composite structures under uniaxial and biaxial loading. *Journal of Nondestructive Evaluation* 29(3): 181–188.

Liu Y, Yekani Fard M, Chattopadhyay A, et al. (2012) Damage assessment of CFRP composites using time-frequency approach. *Journal of Intelligent Material Systems and Structures* 23(4): 397–413.

Lynch JP (2007) An overview of wireless structural health monitoring for civil structures. *Philosophical Transactions of the Royal Society A-Mathematical Physical and Engineering Sciences* 365: 345–372.

Meo M and Zumpano G (2005) Nonlinear elastic wave spectroscopy identification of impact damage on a sandwich plate. *Composite Structures* 71(3–4): 469–474.

Moll J, Schulte RT, Hartmann B, Fritzen C-P and Nelles O (2010) Multi-site damage localization in anisotropic plate-like structures using an active guided wave structural health monitoring system. *Smart Materials and Structures* 19(4): 045022 (16pp.).

Mujica LE, Rodellar J, Fernandez A, et al. (2011) Q-statistic and T^2-statistic PCA-based measures for damage assessment in structures. *Structural Health Monitoring* 10(5): 539–553.

Raghavan A and Cesnik CES (2007) Review of guided-wave structural health monitoring. *The Shock and Vibration Digest* 39(2): 91–114.

Scholkopf B, Smola A and Muller KR (1999) Kernel principal component analysis. In: Scholkopf B, Burges CJC and Smola AJ (eds) *Advances in Kernel Methods—Support Vector Learning*. Cambridge, MA: MIT Press, pp. 327–352.

Seaver M, Aktas E and Trickey ST (2010) Quantitative detection of low energy impact damage in a sandwich composite wing. *Journal of Intelligent Material Systems and Structures* 21(3): 291–308.

Sohn H (2007) Effects of environmental and operational variability on structural health monitoring. *Philosophical Transactions of the Royal Society A-Mathematical Physical and Engineering Sciences* 365(1851): 539–560.

Sohn H, Farrar C, Hunter N, et al. (2001) Structural health monitoring using statistical pattern recognition techniques. *Journal of Dynamic Systems Measurement and Control-Transactions of the ASME* 123(4): 706–711.

Su ZQ, Ye L and Lu Y (2006) Guided Lamb waves for identification of damage in composite structures: a review. *Journal of Sound and Vibration* 295(3): 753–780.

Tang HY, Winkelmann C, Lestari W, et al. (2011) Composite structural health monitoring through use of embedded PZT sensors. *Journal of Intelligent Material Systems and Structures* 22: 739–755.

Yekani Fard M, Liu Y and Chattopadhyay A (2011a) Analytical solution for flexural response of epoxy resin materials.

Journal of Aerospace Engineering. Epub ahead of print 21 May 2011. DOI: 10.1061/(ASCE)AS.1943-5525.0000133.

Yekani Fard M, Liu Y and Chattopadhyay A (2011b) A simplified approach for flexural behavior of epoxy resin materials. *Journal of Strain Analysis for Engineering Design* 47(1): 18–31.

Yekani Fard M, Liu Y and Chattopadhyay A (2012) Characterization of epoxy resin including strain rate effects using digital image correlation system. *Journal of Aerospace Engineering* 24(2): 308–319.